A bump-on-tail model for Alfvén eigenmodes in toroidal plasmas

E Tholerus, T Hellsten and T Johnson

KTH Royal Institute of Technology, School of Electrical Engineering, Department of Fusion Plasma Physics, SE-100 44 Stockholm, Sweden

E-mail: `simon.tholerus@ee.kth.se`

Abstract. Presented is a numerical model for solving the nonlinear dynamics of Alfvén eigenmodes and energetic ions self-consistently. The model is an extension of a previous bump-on-tail model [1, 2], taking into account particle orbits and wave fields in realistic toroidal geometries. The model can be used in conjunction with an orbit averaged Monte Carlo code that handles heating and current drive (similar to e.g. the SELFO code), which enables modeling of the effects of MHD activity on plasma heating. For rapid particle tracing, the unperturbed guiding center orbits are described with canonical action-angle coordinates [3], and the perturbed Hamiltonian for wave-particle interaction is included as Fourier components in the same angles [4]. This allows the numerical integrator to take time steps over several transit periods, which efficiently resolves the relevant time scales for nonlinear wave-particle dynamics. The wave field is modeled by a static eigenfunction and a dynamic complex amplitude driven by the interactions with resonant and non-resonant particles.

1. Introduction

FoxTail ("FOurier series eXpansion of fasT particle-Alfvén eigenmode Interaction"-modeL) is a code that is currently being developed for studying the nonlinear interaction between Alfvén eigenmodes and an energetic distribution of particles in a tokamak plasma. It is a hybrid magnetohydrodynamic-gyrokinetic code that simulates the nonlinear dynamics of the amplitudes of individual eigenmodes and of discrete markers in five-dimensional phase space representing the energetic distribution.

The excitation of toroidal Alfvén eigenmodes is known to cause significant losses in experiments as the wave fields eject energetic ions from the plasma before the ions are being thermalized [5, 6]. In e.g. ICRH scenarios, these modes are often excited by an ensemble of *trapped* energetic ions [7], with an inverted energy distribution along the characteristics of wave-particle interaction in momentum space. FoxTail is initially designed only to describe the dynamics of energetic trapped particles. Only modeling trapped particles with a one-to-one mapping from a set of adiabatic invariants to a particle orbit (category V- and VII-orbits in Ref. [8]) is analytically simpler, since one then avoids possible complications with topological transitions of orbits.

2. Model description

2.1. Brief overview of the code

The FoxTail code consists of two distinct parts, named Fox (FOurier series eXpansion) and Tail (fasT particle-Alfvén eigenmode Interaction modeL). Fox can be viewed as a preprocessor of Tail, and it calculates all the essential data concerning wave-particle interaction for a given equilibrium field configuration. This data is then sent to the Tail code, which solves the nonlinear dynamics of the complete system of Alfvén eigenmodes and energetic particles using Monte Carlo methods. The wave field is mathematically treated as a weak perturbation of the equilibrium system.

The strength of wave-particle interactions depends both on the velocity difference between the particle and the wave phase and on the shape of the orbit relative to the spatial structure of the wave field. The latter is characterized by Fourier coefficients in a transformed poloidal coordinate $\tilde{\theta}$, which is an action-angle coordinate of the equilibrium system [3]. This allows us to reduce the differential equations describing wave-particle interaction to a simple one-dimensional bump-on-tail model [4]. FoxTail is based on this formalism, but it is extended to include a more advanced tracing of the canonical angle coordinates of the particles.

The wave-particle data sent from Fox to Tail is tabulated on a grid in $\boldsymbol{J} \equiv (W, \Lambda, P_\phi)$ space, where W is the particle energy, Λ is the normalized magnetic moment and P_ϕ is the toroidal canonical momentum. All wave-particle data is then interpolated onto the positions of the individual markers in $\boldsymbol{J}$ space. Hence, the domain of the chosen $\boldsymbol{J}$ grid should encompass all markers at all times in the Tail simulations.

Input for the Tail code is also an initial distribution of markers in five dimensional phase space and initial amplitudes and phases of the eigenmodes included to the system. The spatial structures of the eigenmodes and the equilibrium field configuration are assumed to be constant in time throughout the Tail simulations. Therefore, only the amplitudes and phases of the eigenmodes are allowed to vary.

2.2. Action-angle coordinates

The phase space of markers used in Tail are partly described with so called action-angle coordinates of the equilibrium system [3]. They correspond to a particular choice of canonical coordinates that result in very simple equations of motion: all the action-coordinates (momentum space) are constants of motion, and the angle coordinates (configuration space) evolve with constant velocities. In an axisymmetric toroidal plasma with slowly varying electromagnetic fields, one set of action-angle coordinates is $(P_\alpha, \tilde{\alpha}; P_\theta, \tilde{\theta}; P_\phi, \tilde{\phi})$, where $P_\alpha = M\mu/e = M^2 v_\perp^2/(2eB)$, P_θ is the poloidal canonical momentum averaged over the transit orbit (proportional to the toroidal magnetic flux that the orbit encloses in the poloidal plane), and $\tilde{\alpha}$, $\tilde{\theta}$ and $\tilde{\phi}$ are the gyro-angle, poloidal angle and toroidal angle, respectively, interpolated in time across one transit orbit. There exists a mapping between $\boldsymbol{P} \equiv (P_\alpha, P_\theta, P_\phi)$ and $\boldsymbol{J} \equiv (W, \Lambda, P_\phi)$. FoxTail uses

$\boldsymbol{J}$ to describe the momentum space of particles and $(\tilde{\theta}, \tilde{\phi})$ to describe the configuration space ($\tilde{\alpha}$ is ignored, since cyclotron frequencies are assumed to be large). The angle coordinates are mathematically described as

$$\tilde{\theta}(\theta, \boldsymbol{J}) = \int_0^\theta \mathrm{d}\vartheta \, \frac{\omega_{\mathrm{B}}(\boldsymbol{J})}{\dot{\theta}(\vartheta, \boldsymbol{J})}, \; \tilde{\phi}(\theta, \phi, \boldsymbol{J}) = \phi + \int_0^\theta \mathrm{d}\vartheta \, \frac{\omega_{\mathrm{p}}(\boldsymbol{J}) - \dot{\phi}(\vartheta, \boldsymbol{J})}{\dot{\theta}(\vartheta, \boldsymbol{J})}, \tag{1}$$

where the dotted quantities are instantaneous angular velocities of the untransformed coordinates, ω_{B} is the bounce frequency, and ω_{p} is the precession frequency. The above integrals are evaluated along the θ coordinates of the guiding center orbit. FOX numerically calculates the (untransformed) poloidal coordinates $\theta(\tilde{\theta}, \boldsymbol{J})$ and the shifted toroidal coordinates $\phi_{\mathrm{s}}(\tilde{\theta}, \boldsymbol{J}) \equiv \phi - \tilde{\phi} + \omega_{\mathrm{p}}\tilde{\theta}/\omega_{\mathrm{B}}$ for a given set of orbits in $\boldsymbol{J}$ space.

2.3. Orbit solver

The FOX code contains subroutines that solves the 3D motion of trapped particles in a given equilibrium magnetic field configuration on a defined grid in $\boldsymbol{J}$ space. The equilibrium configuration and the particle orbits are described in (ψ, θ, ϕ) space, where ψ is the poloidal magnetic flux (divided by 2π) and θ and ϕ are the untransformed poloidal and toroidal coordinates, respectively. The equilibrium configuration is assumed to be axisymmetric, and the covariant toroidal component of the magnetic field only depends on ψ, according to

$$\boldsymbol{B} = F(\psi)\nabla\phi + \nabla\phi \times \nabla\psi. \tag{2}$$

In order to derive the guiding center orbits in the absence of collisions and wave fields, the adiabatic invariants W, Λ and P_ϕ can be assumed to be exact invariants. Λ and P_ϕ are given by

$$\Lambda = \frac{B_0 v_\perp^2}{B(\psi, \theta) v^2}, \tag{3}$$

$$P_\phi = M\langle v_\phi \rangle_{\mathrm{g}} + eA_\phi = \frac{M v_\parallel F(\psi)}{B(\psi, \theta)} + M v_{\mathrm{d},\phi} - e\psi, \tag{4}$$

where B_0 is the magnetic field strength on the magnetic axis, ψ and θ are the guiding center positions in the poloidal plane, and $\langle \cdot \rangle_{\mathrm{g}}$ averages over the gyro-angle. The lower ϕ index denotes the covariant component of the corresponding vector ($v_\phi = \boldsymbol{v} \cdot \partial \boldsymbol{r}/\partial\phi = R\boldsymbol{v} \cdot \hat{\phi}$). The drift velocity $\boldsymbol{v}_{\mathrm{d}}$ is the combined $\boldsymbol{E} \times \boldsymbol{B}$, ∇B and curvature drifts:

$$\boldsymbol{v}_{\mathrm{d}} = \frac{\boldsymbol{E} \times \boldsymbol{B}}{B^2} + \frac{W(2B_0 - \Lambda B)}{eB_0 B^3} \boldsymbol{B} \times \nabla B. \tag{5}$$

The spatial structure of the orbit in the poloidal plane i solved numerically from the equation $f(\psi, \theta, \boldsymbol{J}) = 0$, where

$$f(\psi, \theta, \boldsymbol{J}) \equiv \frac{\Lambda B(\psi, \theta)}{B_0} - 1 + \frac{B^2(\psi, \theta)[P_\phi + e\psi - M v_{\mathrm{d},\phi}(\psi, \theta, W, \Lambda)]^2}{2MWF^2(\psi)}. \tag{6}$$

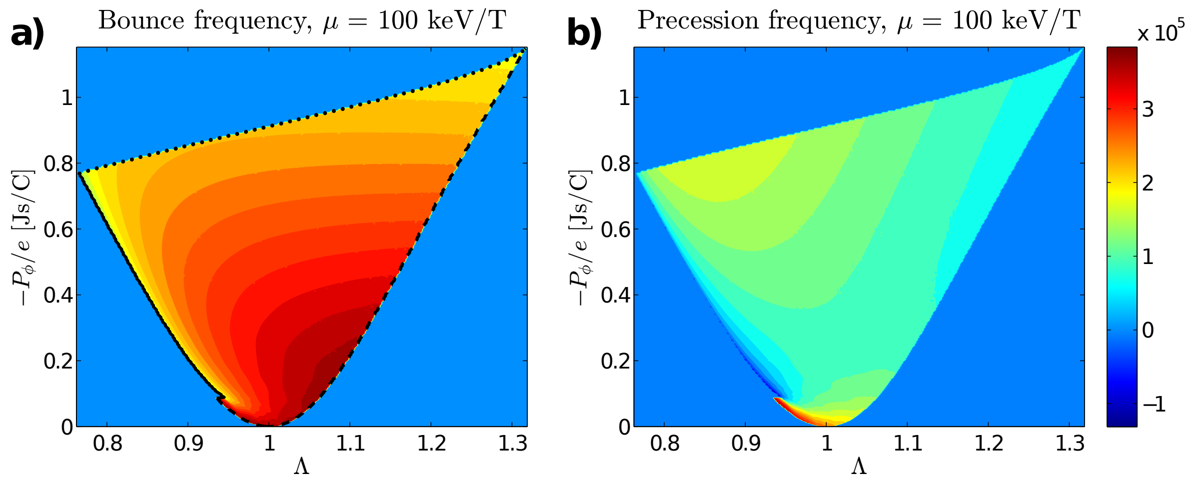

Figure 1. Color coded areas are a) the bounce frequency and b) the precession frequency. The solid curve marks the bifurcation into two orbits, the dashed curve marks where the turning points are in the equatorial mid-plane, and the dotted lines are orbits tangent to the last flux surface.

The output from this part of the code is a coordinate set (ψ_j, θ_j) for each grid point $\boldsymbol{J}_p$, where $j : 0 \to N_p$, and $(\psi_{N_p}, \theta_{N_p}) = (\psi_0, \theta_0)$ is the point where the outer leg of the orbit intersects with the equatorial mid-plane.

The time dependence of the orbit is evaluated from the integral

$$t_j = \int_{\psi_0}^{\psi_j} \frac{\mathrm{d}\psi}{\dot{\psi}} \approx 2 \sum_{k=1}^{j} \frac{\psi_k - \psi_{k-1}}{\dot{\psi}_k + \dot{\psi}_{k-1}}, \;\; \dot{\psi}_j = \boldsymbol{v}_\mathrm{d} \cdot \nabla\psi|_{(\psi_j,\theta_j)} \tag{7}$$

The approximation in eq. (7) is found by assuming $\ddot{\psi}(t)$ to be constant in time between each set of adjacent points (ψ_j, θ_j) and $(\psi_{j+1}, \theta_{j+1})$ along the orbit, and assuming that $\psi(t)$ and $\dot{\psi}(t)$ are continuous. The transformed poloidal coordinates of the orbit are directly evaluated from t_j as $\tilde{\theta}_j = 2\pi t_j / t_{N_p}$. The shifted toroidal coordinates, $\phi_\mathrm{s} \equiv \phi - \tilde{\phi} + \omega_\mathrm{p}\tilde{\theta}/\omega_\mathrm{B}$, are found from the integral

$$\phi_{\mathrm{s},j} = \int_0^{t_j} \mathrm{d}t\, \dot{\phi} \approx \frac{1}{2} \sum_{k=1}^{j} (t_k - t_{k-1})(\dot{\phi}_k + \dot{\phi}_{k-1}), \;\; \dot{\phi}_j = \frac{P_\phi + e\psi_j}{MR^2(\psi_j, \theta_j)}. \tag{8}$$

FOX also requires evaluation of $\dot{\theta}$ at each point along the orbit. They are given by

$$\dot{\theta}_j = \left[\frac{v_\parallel \boldsymbol{B} \cdot \nabla\theta}{B} + \boldsymbol{v}_\mathrm{d} \cdot \nabla\theta \right]_{(\psi_j,\theta_j)} = \left[\frac{J(P_\phi + e\psi - M v_{\mathrm{d},\phi})}{MF} + v_\mathrm{d}^\theta \right]_{(\psi_j,\theta_j)}, \tag{9}$$

where $J \equiv (\nabla\psi \times \nabla\theta) \cdot \nabla\phi$ is the Jacobian.

Presented in Fig. 1 are the calculated bounce frequencies $\omega_\mathrm{B} = 2\pi/t_{N_p}$ and precession frequencies $\omega_\mathrm{p} = \phi_{\mathrm{s},N_p}/t_{N_p}$ in the $\mu = 100$ keV/T plane of $\boldsymbol{J}$ space for a deuterium ion. A simplified equilibrium configuration has been used, with flux surfaces being concentric circles in the poloidal plane. In this parameter regime, ω_B is typically much larger than ω_p, although, they are comparable for $\Lambda \lesssim 1$, $-P_\phi/e \lesssim 0.1$ in the presented test case. The ω_p = const. curves in Fig. 1.b are the curves where the resonance surfaces of the eigenmodes intersect with the $\mu = 100$ keV/T surface.

2.4. Wave field description

The FoxTail model can be used to describe any discrete wave mode with a quasi-static spatial structure. In the following sections, it is shown explicitly how to describe nonlinear interactions with toroidal Alfvén eigenmodes (TAEs). The TAE is a shear Alfvén wave, which can be described by a single scalar potential $\Phi(\boldsymbol{r},t)$ in a low-β plasma [4, 9]. In a toroidal axisymmetric plasma, the scalar potential of each individual eigenmode (indexed by i) can be written on the form

$$\Phi_i(\boldsymbol{r},t) = \sum_m C_i(t)\mathrm{e}^{-\mathrm{i}\chi_i(t)}\Phi_{i,m}(\psi)\mathrm{e}^{\mathrm{i}(n_i\phi - m\theta - \omega_i t)}, \tag{10}$$

where n_i is the toroidal mode number, ω_i is the eigenfrequency, $\Phi_{i,m}(\psi)$ are complex valued eigenfunctions, and C_i and χ_i are real valued, slowly varying amplitude and phase of the mode, respectively ($\dot{C}/C \ll \omega_i$ and $\dot{\chi}_i \ll \omega_i$). The relevant set of eigenmodes to include in Tail simulations depends on the initial distribution of markers (typically, far-from-resonant modes can be disregarded). Note that the transformation $\Phi_{i,m} \to a\Phi_{i,m}$, $C_i \to C_i/a$ for any constant a does not affect Φ_i. We will return to this degree of freedom in Section 2.6. The electric wave field is derived from Φ_i according to [9]

$$\delta\boldsymbol{E} = -\,\mathrm{Re}\sum_i \nabla_\perp\Phi_i = \mathrm{Re}\sum_i C_i\mathrm{e}^{-\mathrm{i}\chi_i}\tilde{\boldsymbol{E}}_i(\boldsymbol{r})\mathrm{e}^{\mathrm{i}(n_i\phi-\omega_i t)}, \tag{11}$$

$$\tilde{\boldsymbol{E}}_i(\boldsymbol{r}) = \sum_m \left(-\frac{\mathrm{d}\Phi_{i,m}}{\mathrm{d}\psi}\nabla\psi + \frac{\mathrm{i}\Phi_{i,m}}{R^2B^2}(mF + n_iB_\theta)(F\nabla\theta - R^2J\nabla\phi)\right)\mathrm{e}^{-\mathrm{i}m\theta}. \tag{12}$$

For the general wave problem, not restricted to TAEs in a low-β plasma, eq. (12) should also contain contributions from e.g. magnetic compression. We choose to apply a Fourier series expansion of $\tilde{\boldsymbol{E}}_i$ also in ψ space:

$$\tilde{\boldsymbol{E}}_i(\boldsymbol{r}) = \sum_{k_\psi,m} \boldsymbol{E}_{i,k_\psi,m}\mathrm{e}^{\mathrm{i}(k_\psi\psi - m\theta)}. \tag{13}$$

This formulation will be useful when deriving the gyrokinetic formulation of the model.

Methods to find approximate solutions of the eigenfunctions $\Phi_{i,m}(\psi)$ from a given equilibrium field configuration in different limits are described e.g. in Refs. [10–12]. In the long term, the code is to be integrated with a code that solves the eigenfunctions $\Phi_{i,m}(\psi)$ and eigenfrequencies ω_i numerically, but the approximate analytical solutions described in the aforementioned references are planned to be used initially.

2.5. Fourier series expansion of Alfvén eigenmode-particle interactions

In order to describe the particle dynamics driven by the wave modes, we first study the work that the wave performs on the particle:

$$\dot{W}(t) = e\boldsymbol{v}(t)\cdot\delta\boldsymbol{E}(\boldsymbol{r}(t),t) \approx e\langle\boldsymbol{v}\cdot\delta\boldsymbol{E}\rangle_\mathrm{g}, \tag{14}$$

where $\boldsymbol{v}(t)$ and $\boldsymbol{r}(t)$ contains both gyration and guiding center motion, and $\langle\cdot\rangle_{\rm g}$ averages over gyro-motion. When the distance between the guiding center position and the magnetic axis is much larger than the Larmor radius, the total particle motion can be approximated by $(\psi(t),\theta(t),\phi(t)) \approx \langle(\psi,\theta,\phi)\rangle_{\rm g} + (\rho_\psi\cos\alpha, \rho_\theta\cos(\alpha+\beta), \rho_\phi\sin\alpha)$, where $\alpha = \alpha_0 + \omega_{\rm c}t$ is the gyro-angle, and $\tan\beta = FJ/(g^{\psi\theta}B)$. Then, the averaged $\boldsymbol{v}\cdot\delta\boldsymbol{E}$ is

$$\langle\boldsymbol{v}\cdot\delta\boldsymbol{E}\rangle_{\rm g} = \langle\boldsymbol{v}\rangle_{\rm g}\cdot{\rm Re}\sum_{i,k_\psi,m} C_i{\rm e}^{-{\rm i}\chi_i}\boldsymbol{E}_{i,k_\psi,m}K_{k_\psi,m,n_i}{\rm e}^{{\rm i}(\langle k_\psi\psi - m\theta + n_i\phi\rangle_{\rm g} - \omega_i t)} + \frac{\mu}{e}\frac{\partial\langle\delta B_\parallel\rangle_{S_{\rm g}}}{\partial t}, \quad (15)$$

$$K_{k_\psi,m,n}(\psi,\theta,\boldsymbol{J}) \equiv \sum_{u,v} J_u(k_\psi\rho_\psi)J_v(m\rho_\theta)J_{u+v}(n\rho_\phi){\rm e}^{-{\rm i}([u-v]\pi/2 - v\beta)} \quad (16)$$

where $J_u(z)$ is the u:th Bessel function of the first kind and $\langle\delta B_\parallel\rangle_{S_{\rm g}}$ is the parallel magnetic wave field component, averaged over the surface enclosed by the gyro-motion. For shear Alfvén waves, the $\delta B_\parallel$ term of eq. (15) is typically negligible. Combining eqs. (14) and (15) and neglecting the $\delta B_\parallel$ term yields

$$\dot{W} = e\,{\rm Re}\sum_i C_i{\rm e}^{-{\rm i}\chi_i}V_i{\rm e}^{{\rm i}(n_i\langle\phi\rangle_{\rm g} - \omega_i t)}, \quad (17)$$

$$V_i(\psi,\theta,\boldsymbol{J}) = \langle\boldsymbol{v}\rangle_{\rm g}\cdot\langle\tilde{\boldsymbol{E}}_i{\rm e}^{{\rm i}n_i\phi}\rangle_{\rm g}{\rm e}^{-{\rm i}n_i\langle\phi\rangle_{\rm g}} = \langle\boldsymbol{v}\rangle_{\rm g}\cdot\sum_{k_\psi,m}\boldsymbol{E}_{i,k_\psi,m}K_{k_\psi,m,n_i}{\rm e}^{{\rm i}\langle k_\psi\psi - m\theta\rangle_{\rm g}}. \quad (18)$$

By evaluating V_i at each point (ψ_j,θ_j) along the guiding center orbit using numerical interpolation, V_i can be expressed as a function of $\tilde{\theta}$. Equation (17) can then be rewritten in terms of the transformed angle coordinates $(\tilde{\theta},\tilde{\phi})$ according to

$$\dot{W} = {\rm Re}\sum_{i,\ell} C_i{\rm e}^{-{\rm i}\chi_i}V_{i,\ell}{\rm e}^{{\rm i}(\ell\tilde{\theta} + n_i\tilde{\phi} - \omega_i t)}, \quad (19)$$

$$V_{i,\ell}(\boldsymbol{J}) = \frac{e}{2\pi}\int_0^{2\pi} d\tilde{\theta}\, V_i(\tilde{\theta},\boldsymbol{J})\exp\left[{\rm i}\left(n_i\left[\phi_{\rm s}(\tilde{\theta},\boldsymbol{J}) - \frac{\omega_{\rm p}(\boldsymbol{J})}{\omega_{\rm B}(\boldsymbol{J})}\tilde{\theta}\right] - \ell\tilde{\theta}\right)\right]. \quad (20)$$

The coefficients $V_{i,\ell}$ are the Fourier series expansion of the Alfvén eigenmode-particle interaction that named the FOX code. For efficient calculation of $\dot{W}$ in simulations with the TAIL code, the Fourier series are truncated at a given $|\ell| = \ell_{\rm max}$. For TAEs, resonant energetic particles typically satisfy $\omega_{\rm p} \sim \omega_i/n_i$ and $\omega_{\rm B} \gg \omega_i$, meaning that mainly the $\ell = 0$ term of eq. (17) contributes on time scales $\gg \omega_{\rm B}^{-1}$. Note that close to the trapped-passing boundary, where $\omega_{\rm p}/\omega_{\rm B} \to \infty$, the integrand of eq. (20) oscillates infinitely fast in $\tilde{\theta}$, resulting in $V_{i,\ell} \to 0$ for $|\ell| \ll |n_i\omega_{\rm p}/\omega_{\rm B}|$ when approaching this boundary.

2.6. Modeling wave-particle interaction (TAIL code)

The wave-particle system can be described by a single Hamiltonian, where the pairs $(P_\alpha,\tilde{\alpha})$, $(P_\theta,\tilde{\theta})$, $(P_\phi,\tilde{\phi})$ and $(C_i^2/(2\omega_i),\chi_i)$ are canonically conjugate pairs (see e.g. Refs. [3,4] for details). Choosing $C_i^2/(2\omega_i)$ and χ_i to be canonically conjugate defines the normalization of $\Phi_{i,m}$ and C_i that was mentioned in Section 2.4. The total Hamiltonian is

$$\mathcal{H} = \sum_k \Big[\mathcal{H}_0(\boldsymbol{P}_k) + \sum_i \mathcal{H}_1(\boldsymbol{P}_k, \tilde{\theta}_k, \tilde{\phi}_k, C_i^2/(2\omega_i), \chi_i, t)\Big], \tag{21}$$

where k is the marker index, i is mode index, $\boldsymbol{P} \equiv (P_\alpha, P_\theta, P_\phi)$, and $\mathcal{H}_1 \ll \mathcal{H}_0$. The equilibrium Hamiltonian $\mathcal{H}_0$ satisfies $\partial\mathcal{H}_0/\partial\boldsymbol{P} = (\bar{\omega}_\mathrm{c}, \omega_\mathrm{B}, \omega_\mathrm{p})$, where $\bar{\omega}_\mathrm{c}$ is the gyro-frequency, averaged over the transit orbit. The perturbation Hamiltonian $\mathcal{H}_1$ is

$$\mathcal{H}_1 = \int^t \mathrm{d}t'\, \dot{W}(\boldsymbol{P}, \tilde{\theta}, \tilde{\phi}, C_i^2/(2\omega_i), \chi_i, t') = -\,\mathrm{Im}\sum_\ell \frac{1}{\omega_i} C_i \mathrm{e}^{-\mathrm{i}\chi_i} V_{i,\ell}(\boldsymbol{P}) \mathrm{e}^{\mathrm{i}(\ell\tilde{\theta} + n_i\tilde{\phi} - \omega_i t)}. \tag{22}$$

$P_\alpha = M\mu/e = M\Lambda W/(eB_0)$ is a constant of motion also in the wave-particle system, since $\dot{W}$ in eq. (19) is independent of the transformed gyration angle $\tilde{\alpha}$. From the perturbation Hamiltonian in eq. (22), one can derive the equations of motion of the wave-particle system:

$$\begin{cases} \mathrm{d}W_k = \mathrm{Re}\sum_i A_i U_{i,k}\mathrm{d}t, & \mathrm{d}A_i = -\sum_k w_k U_{i,k}^*\mathrm{d}t, \\ \mathrm{d}(\Lambda_k W_k) = 0, & \mathrm{d}\tilde{\theta}_k = \omega_\mathrm{B}(\boldsymbol{J}_k)\mathrm{d}t + \left.\dfrac{\partial\tilde{\theta}}{\partial\boldsymbol{J}}\right|_{(\tilde{\theta}_k, \boldsymbol{J}_k)} \cdot \mathrm{d}\boldsymbol{J}_k, \\ \mathrm{d}P_{\phi,k} = \mathrm{Re}\sum_i \dfrac{n_i}{\omega_i} A_i U_{i,k}\mathrm{d}t, & \mathrm{d}\tilde{\phi}_k = \omega_\mathrm{p}(\boldsymbol{J}_k)\mathrm{d}t + \left.\dfrac{\partial\tilde{\phi}}{\partial\boldsymbol{J}}\right|_{(\tilde{\theta}_k, \boldsymbol{J}_k)} \cdot \mathrm{d}\boldsymbol{J}_k, \end{cases} \tag{23}$$

where $A_i \equiv C_i \mathrm{e}^{-\mathrm{i}\chi_i}$, and

$$U_{i,k} \equiv \sum_{\ell=-\ell_\mathrm{max}}^{\ell_\mathrm{max}} V_{i,\ell}(\boldsymbol{J}_k) \mathrm{e}^{\mathrm{i}(\ell\tilde{\theta}_k + n_i\tilde{\phi}_k - \omega_i t)}. \tag{24}$$

Weight factors w_k have been introduced, which lets the k:th marker represent a set of w_k particles. Additional operators to model e.g. particle collisions or RF heating may be added to $\mathrm{d}\boldsymbol{J}_k$. The total energy of the wave-particle system,

$$W_\mathrm{tot} = \sum_k w_k W_k + \sum_i \frac{|A_i|^2}{2} \tag{25}$$

is a global constant of motion in the absence of applied sources and sinks. Hence, the eigenfunctions $\Phi_{i,m}$ and amplitudes C_i are normalized such that $|A_i|^2/2 = C_i^2/2$ is the total energy of the wave mode.

Note that the phase equations of eq. (23) contain terms depending on $\mathrm{d}\boldsymbol{J}_k$. These terms appear since $\tilde{\theta}$ and $\tilde{\phi}$ depend on $\boldsymbol{J}$, see eq. (1). The derivatives $\partial\tilde{\theta}/\partial\boldsymbol{J}$ and $\partial\tilde{\phi}/\partial\boldsymbol{J}$ are evaluated while keeping θ and ϕ constant. Once $\partial\tilde{\theta}/\partial\boldsymbol{J}$ is found, $\partial\tilde{\phi}/\partial\boldsymbol{J}$ is calculated as

$$\frac{\partial\tilde{\phi}}{\partial\boldsymbol{J}} = \tilde{\theta}\frac{\partial}{\partial\boldsymbol{J}}\left(\frac{\omega_\mathrm{p}}{\omega_\mathrm{B}}\right) + \left(\frac{\omega_\mathrm{p}}{\omega_\mathrm{B}} - \frac{\partial\phi_\mathrm{s}}{\partial\tilde{\theta}}\right)\frac{\partial\tilde{\theta}}{\partial\boldsymbol{J}} - \frac{\partial\phi_\mathrm{s}}{\partial\boldsymbol{J}} \tag{26}$$

Approximations of $\partial\tilde{\theta}/\partial\boldsymbol{J}$ and $\partial\tilde{\phi}/\partial\boldsymbol{J}$ can be found by expressing them as functions of $(\tilde{\theta}, \boldsymbol{J})$ and making Fourier series expansions in $\tilde{\theta}$ space:

$$\frac{\partial\tilde{\theta}}{\partial\boldsymbol{J}} \approx \sum_{q=-q_\mathrm{max}}^{q_\mathrm{max}} \boldsymbol{X}_q(\boldsymbol{J})\mathrm{e}^{\mathrm{i}q\tilde{\theta}},\ \frac{\partial\tilde{\phi}}{\partial\boldsymbol{J}} \approx \sum_{q=-q_\mathrm{max}}^{q_\mathrm{max}} \boldsymbol{Y}_q(\boldsymbol{J})\mathrm{e}^{\mathrm{i}q\tilde{\theta}}. \tag{27}$$

When $\boldsymbol{X}_q(\boldsymbol{J}(t))$ and $\boldsymbol{Y}_q(\boldsymbol{J}(t))$ evolve on time scales much longer than ω_{B}^{-1} (that is, when the orbit shapes are essentially unchanged on time scales ω_{B}^{-1}), the terms with $|q| \geq 1$ are asymptotically small. Furthermore, when there is up-down symmetry of the equilibrium field configuration, it can be shown that $\boldsymbol{X}_0 = \boldsymbol{Y}_0 = \boldsymbol{0}$. Hence, the $\mathrm{d}\boldsymbol{J}_k$ terms of $\mathrm{d}\tilde{\theta}_k$ and $\mathrm{d}\tilde{\phi}_k$ in eq. (23) is expected to be most relevant when the shape of the orbit is rapidly varied (for instance, in topological orbit transitions) or when there is up-down asymmetry. When $\mathrm{d}\boldsymbol{J}_k$ contains diffusion terms, e.g. due to collisions, the $\mathrm{d}\boldsymbol{J}_k$ terms of $\mathrm{d}\tilde{\theta}_k$ and $\mathrm{d}\tilde{\phi}_k$ in eq. (23) corresponds to so called *phase decorrelation*, which is thoroughly studied in Refs. [1,2]. It was shown in these references that a relatively weak phase decorrelation (phase decorrelation times longer than the growth rate of the wave amplitude) is required to strongly affect the macroscopic dynamics of the system.

Tail will solve the set of differential equations in eq. (23) numerically, e.g. by using a Runge-Kutta algorithm. The following data is required from the Fox code for all the grid points $\boldsymbol{J}_p$: $V_{i,\ell}$, ω_{B}, ω_{p}, $\boldsymbol{X}_q$ and $\boldsymbol{Y}_q$. The Tail code also requires information about the eigenfrequencies ω_i and the toroidal mode numbers n_i of all included eigenmodes. Furthermore, Fox outputs parametrizations of the topological boundaries of the orbits in $\boldsymbol{J}$ space, and the boundary where the outer leg of the orbit passes the last flux surface, ψ_{edge}. These parametrizations are then used to properly apply boundary conditions in Tail. Besides the output from Fox, the solver requires an initial distribution of markers in $(\tilde{\theta}, \tilde{\phi}, \boldsymbol{J})$ space and initial complex amplitudes A_i of each simulated eigenmode. Solving the differential equations of eq. (23) using time steps larger than or similar to ω_{B}^{-1} can only be done as long as the $\tilde{\theta}$ coordinate can be ignored in simulations, that is, if it is sufficient to set $\ell_{\max} = q_{\max} = 0$.

In initial versions of the model, which only simulate trapped particles, artificial boundary conditions need to be applied to the system in order to prevent markers from entering the regions of $\boldsymbol{J}$ space where there are passing orbits and/or bifurcating orbit solutions (dashed and solid curves in Fig. 1.a). We propose to deal with these boundaries by letting the interaction strength with the wave modes decay to zero towards the boundary. Markers with orbits that cross the last flux surface (dotted curve in Fig. 1.a) are considered lost and removed from the simulations.

3. Summary

This paper presents the mathematical description of a magnetohydrodynamic-gyrokinetic model that self-consistently solves the nonlinear dynamics of energetic particles interacting with a set of Alfvén eigenmodes in a toroidal plasma. In the model, the wave fields are treated as weak perturbations of the equilibrium system. The strength of wave-particle interaction due to the spatial structure of the particle orbit relative to the wave fields is characterized by a set of Fourier coefficients [4] in the poloidal action-angle coordinate of the equilibrium system [3]. It is explicitly shown how the dynamics of toroidal Alfvén eigenmodes (TAEs) are solved, but the model can describe systems with any discrete wave modes with quasi-static spatial structures. The presented mathematical description allows for efficient resolution of the relevant wave-particle dynamics, since one does not need to resolve bounce time scales of energetic particles. Direct perturbations of the phase coordinates of the particles due to the perturbation of momentum coordinates W, Λ and P_ϕ, are quantitatively described. These perturbations can be used to model phase decorrelation [1,2], e.g. due to collisions.

References

[1] Tholerus E, Hellsten T and Johnson T 2015 *Phys. Plasmas* **22** 082106

[2] Tholerus S, Hellsten T and Johnson T 2014 *J. Phys.: Conf. Ser.* **561** 012019

[3] Kaufman A N 1972 *Phys. Fluids* **15** 1063

[4] Berk H L, Breizman B N and Pekker M S 1995 *Nucl. Fusion* **35** 1713

[5] Heidbrink W W, Strait E J, Doyle E, Sager G and Snider R T 1991 *Nucl. Fusion* **31** 1635

[6] Wong K L *et al* 1991 *Phys. Rev. Lett.* **66** 1874

[7] Sandquist P, Sharapov S E, Lisak M, Johnson T and JET-EFDA contributors 2007 *Phys. Plasmas* **14** 122506

[8] Hedin J, Hellsten T, Eriksson L G and Johnson T 2002 *Nucl. Fusion* **42** 527

[9] Berk H L, Van Dam J W, Guo Z and Lindberg D M 1992 *Phys. Fluids B* **4** 1806

[10] Cheng C Z and Chance M S 1986 *Phys. Fluids* **29** 3695

[11] Candy J, Breizman B N, Van Dam J W and Ozeki T 1996 *Phys. Lett. A* **215** 299

[12] Rosenbluth M N, Berk H L, Van Dam J W and Lindberg D M 1992 *Phys. Fluids B* **4** 2189